

Short communication

Static optimal estimation of joint accelerations for inverse dynamics problem solution

Violaine Cahouët^{a,*}, Martin Luc^b, Amarantini David^b

^aLaboratoire Motricité-Plasticité INSERM/ERIT-M 0207, UFRSTAPS, Université de Bourgogne BP 27877, 21078 Dijon, France

^bLaboratoire Sport et Performance Motrice EA 597, Université Joseph Fourier, 38041 Grenoble cedex 9, France

Accepted 21 June 2002

Abstract

In inverse dynamics computations, the accuracy of the solution strongly depends on the accuracy of the input data. In particular, estimated joint moments are highly sensitive to uncertainties in acceleration data. The aim of the present work was to improve classical inverse dynamics computations by providing an accurate estimation of accelerations. Accelerations are usually calculated from noise-polluted position data using numerical double differentiation, which amplifies measurement noise. The objective of the present paper is to use all available imperfect position and force measurements to extract optimum acceleration estimations. A weighted least-squares optimisation approach is used to provide optimal acceleration distributions most consistent with position and force data, and which account for the propagation of measurement uncertainties. The task chosen for comparing the solution methodology with other classical methods is a typical experimental postural movement, consisting in upper limb swings from an upright stance. The proposed method delivers a set of optimal accelerations well consistent with all available measurements. It also leads to an accurate prediction of ground reactions and it produces no residual moment at the top-most segment.

© 2002 Elsevier Science Ltd. All rights reserved.

Keywords: Inverse dynamics; Static optimisation; Net joint moment

1. Introduction

The knowledge of internal forces in multi-articulated human movements is of considerable importance in many biomechanical and neuro-physiological investigations. The estimation of inter-segmental forces and joint moments based on externally measured movements of body segments is referred to as the ‘inverse dynamics problem’.

Traditionally, this problem is addressed by solving iteratively the equations of motion for each body segments using, for example, the mechanical approaches of Newton–Euler or Lagrange (Zajac and Gordon, 1989). This pure inverse dynamics approach (PID) requires only kinematic measurements, but it may generate inaccurate joint moment estimations because the accuracy of the solution strongly depends on the accuracy of input data (Hatze, 2000). In particular, the

computed joint moments are exquisitely sensitive to uncertainties in accelerations data (Cappozzo et al., 1975; Challis and Kerwin, 1996). One modification of this scheme, the so-called ‘bottom-up’ method, is a mixed approach, that also uses ground reaction component recordings (Winter, 1990). Measuring external forces and moment acting on the bottom-most segment reduces the influence of the acceleration estimates, and joint moment estimations tend to be more accurate in the bottom part of the body system (Zajac, 1993). However, the introduction of additional data leads to an over-determined system and this method generates additional residual forces and moment at the top-most segment, where the equilibrium conditions are no longer satisfied.

Alternatively, one can use an optimisation approach. Chao and Rim (1973) applied a dynamic optimisation process to obtain the distributions of joint moments that best reproduced the measured motion in a forward simulation. Kuo (1998) solved the inverse dynamics problem as an over-complete system of equations using a static optimisation approach to find the set of joint

*Corresponding author. Tel.: +33-3-80-39-67-84; fax: +33-3-80-39-67-02.

E-mail address: violaine.cahouet@u-bourgogne.fr (V. Cahouët).

moments that agrees best with accelerations data and force plate measurements. These methods are effective but their implementation requires an advanced knowledge of multi-body dynamics and involves the modification of the traditional solution process for inverse dynamics.

Considering that the problem of inaccuracy in joint moment calculations is closely related to the quality of acceleration estimations (Cappozzo et al., 1975; Challis and Kerwin, 1996), a simpler alternative is to improve the classical inverse dynamics computations by providing an accurate estimation of acceleration values. Accelerations are usually calculated from noise-polluted position data by using numerical double differentiation, which amplifies measurement noise. Low-pass filtering of raw position data improves the accuracy of the double differentiation calculations by reducing high-frequency random measurement noise (Winter, 1990). Nevertheless, data smoothing cannot eliminate systematic errors introduced, for example, by the inaccurate positions of body markers (Wood, 1982). The objective is to use all available imperfect position and force measurements to compute the best possible acceleration estimates. The over-determinacy arising from the introduction of force plate measurements can be used in a static optimisation scheme (Vaughan et al., 1982; Kuo, 1998) to optimise acceleration values.

The aim of this study is to improve inverse dynamics computations by providing better estimations of input acceleration data. A least-squares optimisation approach is used in order to provide optimal acceleration values most consistent with dynamic and kinematic measurements. Joint moments can then be calculated from these optimal kinematic values via inverse dynamics. The relative influence of the inaccuracy of both force and position measurements on acceleration estimation is controlled by introducing a weight matrix into the least-squares formulation. The proposed methodology is critically assessed by comparing the results given by different methods for a typical postural motion consisting of rapid voluntary upper limb swings performed in an upright position. This task has been widely studied in the literature (Eng et al., 1992) and produces a large movement amplitude at the shoulder joint and small postural adjustments at the hip and ankle articulations (Kuo and Zajac, 1993).

2. Methods

2.1. Multibody model

The general configuration of the two-dimensional (2D) system used for solving the inverse dynamic problem is presented in Fig. 1. The model comprises $n + 1$ segments labelled from 0 (feet) to n (top-most

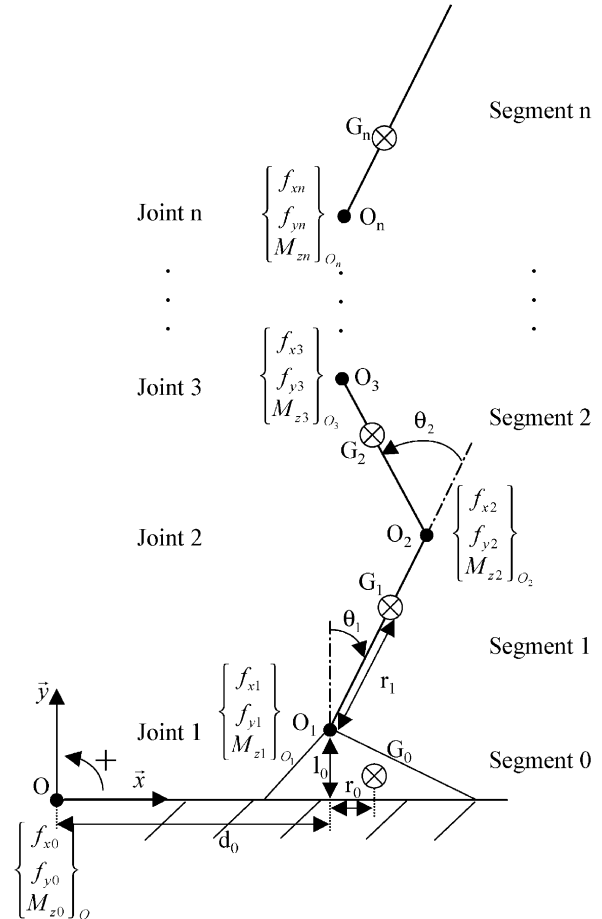


Fig. 1. Configuration of the 2D-body segment model consisting $(n + 1)$ segments linked by n joints. For each segment $i \geq 0$: l_i and m_i are, respectively, the length and the mass, G_i the centre of mass, r_i the distance between G_i and joint i (r_0 is the horizontal distance between G_0 and joint 1) and J_i , the moment of inertia with respect to the axis (G_i, z). For $i \geq 1$: θ_i is the angular orientation with respect to segment $i-1$ (and with respect to the vertical direction for segment $i = 1$). f_{xi}, f_{yi} and M_{zi} are the components of the load vector ϕ_i acting on segment i at joint i , they represent, respectively, the horizontal inter-segmental force, the vertical inter-segmental force, and the net joint torque in O_i . f_{x0}, f_{y0} and M_{z0} are the components of the ground reaction vector ϕ_0 acting on the feet at O .

segment), linked by n joints. The feet remain at rest, in static contact with the force plate.

2.2. Calculation method

The calculation of joint moments is decomposed into two successive steps: the first one yields a least-squares estimation of accelerations from kinematic and dynamic data and in the second step, the inverse dynamics problem, relating joint moments to angular accelerations, is solved.

2.2.1. Least-squares estimation of accelerations

Two sets of equations are needed to characterize the over-complete system.

The first one is a system of three equations describing the static equilibrium of the feet. It is derived from the action-reaction principle expressed at O_1 as

$$\boldsymbol{\varphi}_0 + \boldsymbol{\lambda}_0 = \boldsymbol{\varphi}_1 \quad (1)$$

with $\boldsymbol{\lambda}_0 = \langle 0, -m_0g, l_0f_{x0} - d_0f_{y0} - r_0m_0g \rangle^T$ where d_0 is the horizontal distance between the origin of the force plate O and the ankle joint centre O_1 (see Fig. 1).

Considering the multi-articulated system composed of the n upper segments (1– n), Euler's equations can relate the inter-segmental forces (f_{x1} and f_{y1}) and the net joint moment (M_{z1}) at the ankle joint to the kinematics of the system (Andrews, 1995). f_{x1} and f_{y1} are related to the rate of change of the horizontal and vertical linear momenta of the whole system. Similarly, M_{z1} equals the rate of change of the angular momentum of the entire system. The expression of $\boldsymbol{\varphi}_1$ which describes the kinematics of the whole system at each time t is derived as

$$\boldsymbol{\varphi}_1 = \langle f_{x1}, f_{y1}, M_{z1} \rangle^T = P(\boldsymbol{\theta})\ddot{\boldsymbol{\theta}} + R(\boldsymbol{\theta})\dot{\boldsymbol{\theta}}^2 + T(\boldsymbol{\theta})\dot{\boldsymbol{\theta}}\dot{\boldsymbol{\theta}} + \boldsymbol{\gamma}(\boldsymbol{\theta}), \quad (2)$$

where $\boldsymbol{\theta} = \langle \theta_1, \dots, \theta_n \rangle^T$ is the angular position measurement vector at time t (recorded with the sampling frequency Δf_e), $\ddot{\boldsymbol{\theta}} = \langle \ddot{\theta}_1, \dots, \ddot{\theta}_n \rangle^T$ is the angular acceleration vector, $\dot{\boldsymbol{\theta}}^2$ and $\dot{\boldsymbol{\theta}}\dot{\boldsymbol{\theta}}$ are velocity vectors such that $\dot{\boldsymbol{\theta}}^2 = \langle \dot{\theta}_1^2, \dots, \dot{\theta}_n^2 \rangle^T$ and $\dot{\boldsymbol{\theta}}\dot{\boldsymbol{\theta}} = \langle \dot{\theta}_1\dot{\theta}_2, \dot{\theta}_1\dot{\theta}_3, \dots, \dot{\theta}_{n-1}\dot{\theta}_n \rangle^T$, and $\boldsymbol{\gamma}$ is a gravitational vector defined by

$$\boldsymbol{\gamma}(\boldsymbol{\theta}) = \left\langle 0, \sum_{i=1,n} m_i g, f_g(\boldsymbol{\theta}) \right\rangle^T.$$

where P , R and T are, respectively, the inertial, centrifugal and Coriolis' coefficient matrices, and f_g is a gravitational function (see Appendix A).

Combining Eq. (1) with Eq. (2) produces a system of three equations relating body kinematics and force plate dynamics at each time t :

$$P\ddot{\boldsymbol{\theta}} = \boldsymbol{\varphi}_0 + \boldsymbol{\lambda}_0 + \boldsymbol{\kappa}(\boldsymbol{\theta}), \quad (3)$$

where $\boldsymbol{\kappa}(\boldsymbol{\theta}) = -(\boldsymbol{\gamma}(\boldsymbol{\theta}) + R(\boldsymbol{\theta})\dot{\boldsymbol{\theta}}^2 + T(\boldsymbol{\theta})\dot{\boldsymbol{\theta}}\dot{\boldsymbol{\theta}})$.

A second set of n equations relates the angular acceleration vector $\ddot{\boldsymbol{\theta}}$ to the angular position measurement vector $\boldsymbol{\theta}$:

$$I\ddot{\boldsymbol{\theta}} = \boldsymbol{\delta}(\boldsymbol{\theta}), \quad (4)$$

where I is the $n \times n$ identity matrix, and $\boldsymbol{\delta}(\boldsymbol{\theta})$ is formulated by using a centred finite difference scheme as

$$\boldsymbol{\delta}(\boldsymbol{\theta}) = \frac{\Delta f_e^2}{4} (\boldsymbol{\theta}_{t-2\Delta t} - 2\boldsymbol{\theta} + \boldsymbol{\theta}_{t+2\Delta t}).$$

The resulting over-determined $((n+3) \times n)$ linear system relating the angular acceleration vector to the position and force measurements is obtained from Eqs. (3) and (4). It reads

$$U\ddot{\boldsymbol{\theta}} = \mathbf{s} \quad (5)$$

with

$$U = \begin{bmatrix} P \\ I \end{bmatrix} \quad \text{and} \quad \mathbf{s} = \begin{Bmatrix} (\boldsymbol{\varphi}_0 + \boldsymbol{\lambda}_0 + \boldsymbol{\kappa}(\boldsymbol{\theta})) \\ \boldsymbol{\delta}(\boldsymbol{\theta}) \end{Bmatrix}.$$

In general, there exists no exact solution to this system of equations if the measurements $\boldsymbol{\theta}$ and $\boldsymbol{\varphi}_0$ are noise-polluted. A least-squares estimation may be used in order to obtain the angular accelerations that best agree with position and force measurements.

Propagation of measurement uncertainties:

The right-hand side of system (5) is determined with the experimental values of parameters $f_{x0}, f_{y0}, M_{z0}, \theta_1, \dots, \theta_n$ at different times. The uncertainties of each component of \mathbf{s} due to measurement errors can be quantified by applying the error propagation law suggested by the ISO guide (1993). In particular, assuming all measurements x_k are uncorrelated, the variance of each component s_i is evaluated by (see Appendix B)

$$\Delta s_i^2 = \sum_k \left(\frac{\partial s_i}{\partial x_k} \right)^2 \Delta x_k^2, \quad (6)$$

where Δx_k is the standard uncertainty associated with the measurement x_k . Considering the measurement error E_{xk} due to the resolution of the sensor, the associated uncertainty of x_k can be estimated with (ISO guide, 1993)

$$\Delta x_k = \frac{E_{xk}}{2\sqrt{3}} \quad (7)$$

In order to balance the different uncertainties of \mathbf{s} , a weight matrix W is introduced in the least-squares estimation scheme. Considering all experimental parameters as independent, W is a positive diagonal $(n+3) \times (n+3)$ matrix and the weight coefficients can be chosen such that (Woltring, 1990)

$$w_i = \frac{1}{\Delta s_i^2}. \quad (8)$$

Multiplying Eq. (5) by W , the optimal angular acceleration vector $\hat{\boldsymbol{\theta}}$ is defined at each time t by

$$WU\hat{\boldsymbol{\theta}} - W\mathbf{s} = \underset{\hat{\boldsymbol{\theta}}}{\text{Min}}(WU\ddot{\boldsymbol{\theta}} - W\mathbf{s}), \quad (9)$$

where Min refers to the value of $\hat{\boldsymbol{\theta}}$ that realises the minimisation in the least-squares sense.

The solution $\hat{\boldsymbol{\theta}}$ of the linear Eq. (9) can be obtained by the following $(n \times n)$ system (Ciarlet, 1994)

$$U^T WU\hat{\boldsymbol{\theta}} = U^T W\mathbf{s}. \quad (10)$$

2.2.2. Equations of motion

The inverse dynamics problem is solved by using the Lagrangian formalism (Späegele et al., 1999) and net joint moments are obtained from optimal acceleration values.

2.3. Experimental design

From an initial standing position with the arms in front of the body, the two hands held at shoulder width, the subject (height = 1.82 m, mass = 70 kg) was asked to perform rapid upward and downward symmetrical arm swings. He was requested not to move his feet and to maintain full elbow and knee extensions. All movements were self-initiated and assumed symmetrical.

2.3.1. Instrumentation

Position measurements: Two cameras (sampling frequency of 100 Hz) recorded X and Y movements of retro-reflective markers fixed on anatomical landmarks, using an opto-electronic measuring device ELITE (BTS, Milan, Italy). Five markers were placed on the subject's left side at the following sites: fifth metatarsal head, lateral maleolus (ankle joint), great trochanter (hip joint), acromion (shoulder joint) and wrist. Accuracy was $1/2500$ of the field of view and a resulting average spatial resolution $E_\theta = 1^\circ$ for angular position measurements was estimated (Eq. (7)).

Force and moment measurements: Horizontal (anterior-posterior) (f_{x0}) and vertical (f_{y0}) ground reaction forces and moment (M_{z0}) were obtained from a force platform AMTI (Advanced Mechanical Technology Inc. Watertown, USA) with a sampling frequency of 100 Hz. The measurement errors $E_{f_x} = 1\text{ N}$, $E_{f_y} = 3\text{ N}$ and $E_{M_z} = 3\text{ Nm}$ were estimated from the resolution of the sensors (Eq. (7)).

2.3.2. Data-processing

Force plate measurements and X and Y displacement data of each marker were filtered using a fourth-order Butterworth filter with zero phase lag and a net cut-off frequency of 9 Hz for forces and moment and 6 Hz for positions. Anthropometric data necessary for the calculations were estimated from the height and mass of the subject (Winter, 1990). Inter-segmental angles were calculated at ankle, hip and shoulder joints according to the convention in Fig. 1. Angular velocities were calculated at each time t from filtered angular positions using a centred finite difference scheme

$$\dot{\theta} = \frac{\Delta f_e}{2}(\theta_{t+\Delta t} - \theta_{t-\Delta t}).$$

Inverse dynamics calculations were conducted with a four-link model ($n = 3$), the three joints mainly involved in this task being the ankle, hip and shoulder articulations (knee joints were motionless during the task).

2.4. Data analysis

Accelerations obtained from our method were compared to those from classical numerical differentiation. We compared the ground reaction signals calculated

either from numerical differentiations or from optimal accelerations to the experimental data. Deviations between two signals are quantified by using the square root of the time-averaged squared error, normalized with respect to mean peak-to-peak amplitude:

$$\begin{aligned} & \text{'relative RMS error'} \\ &= \frac{\sqrt{1/T \int_0^T (s_1(t) - s_2(t))^2 dt}}{1/2 \left(\sum_{i=1}^2 (\text{Max}_{0 < t < T}(s_i(t)) - \text{Min}_{0 < t < T}(s_i(t))) \right)} \\ & \times 100\%. \end{aligned} \quad (10')$$

Comparisons between joint moment solutions obtained from 'PID', 'bottom-up' and our method are based on absolute RMS errors.

In what follows, estimations obtained by our method are referred to as 'optimal' solutions.

3. Results

The patterns of the ankle, hip and shoulder angular acceleration calculated by numerical double-differentiation of position data (Eq. (4)) and those given by the proposed method (Eq. (10)) are presented in Fig. 2. The upward and downward arm swings are well identified in the skew-symmetric curves of the shoulder angular accelerations. Skew-symmetric movements are also observed about the two other joints, but with smaller amplitudes. Relative RMS errors associated with position double-differentiation and optimal acceleration calculations at the ankle, hip and shoulder joints are, respectively, 12.2%, 13.0% and 6.2%.

The numerically differentiated and optimal joint angular accelerations are introduced in Eq. (3) in order to obtain the estimations of the ground reaction vector components (Φ_0). The results are compared to each other and to the actual force plate measurements (Fig. 3). The Relative RMS errors between the two calculated solutions for horizontal (f_{x0}) and vertical (f_{y0}) ground reaction forces and moment (M_{z0}) are, respectively, 21.6%, 4.7% and 10.1%. The deviations between the actual plate force measurements and the estimations of f_{x0} , f_{y0} and M_{z0} are, respectively, 38.8%, 4.5% and 9.2% (numerically differentiated accelerations), and 1.5%, 0.05% and 0.1% (optimal accelerations).

Finally, net joint moments were estimated by three different techniques: the classical 'PID' and 'bottom-up' methods using numerically differentiated accelerations and our new procedure. The corresponding joint moments patterns and the residual moment induced by the 'bottom-up' approach are presented in Fig. 4. The Absolute RMS values between optimal solutions and others calculations at ankle, hip and shoulder joints are, respectively, 34.0, 19.9 and 12.9 N m (PID method), and 0.04, 2.6 and 14.0 N m (bottom-up method).

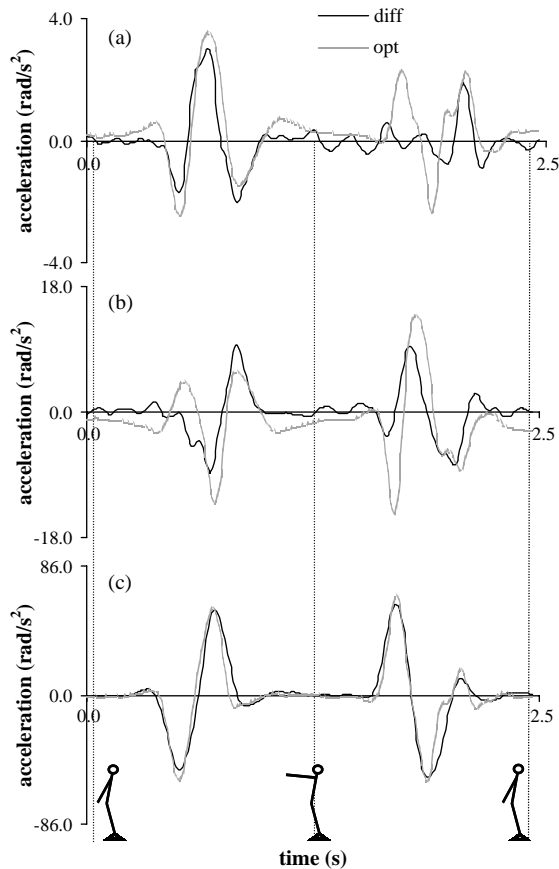


Fig. 2. Accelerations calculated by numerical differentiation of position measurements (diff) and optimal method (opt) at each joint: ankle (a), hip (b) and shoulder (c).

4. Discussion

The mean deviation between optimal acceleration solutions (see Fig. 2) and numerical double-differentiation position measurements is approximately 10%. Even though the two different solutions follow similar patterns at each joint, optimal signals present smoother profiles with high-frequency component with lower amplitude, in the stable periods of the task. In particular, the smaller relative deviation (6.2%) observed at the shoulder joint can be explained by the large arm movement amplitude resulting in minimal relative position measurement errors. For the two other joints, characterized by smaller displacements (postural adjustments) close to the camera resolution, relative errors are more important (12.2% for the ankle joint and 13.0% for the hip joint). Indeed, it can be observed that for the ankle joint angular acceleration, the optimal solution predicts a skew-symmetric acceleration pattern, which does not emerge in the numerically differentiated data. Deviations in the estimations of acceleration can lead to large differences in calculated ground reactions (see Fig. 3). Considering calculated and measured signals, solutions from the proposed method provide the best

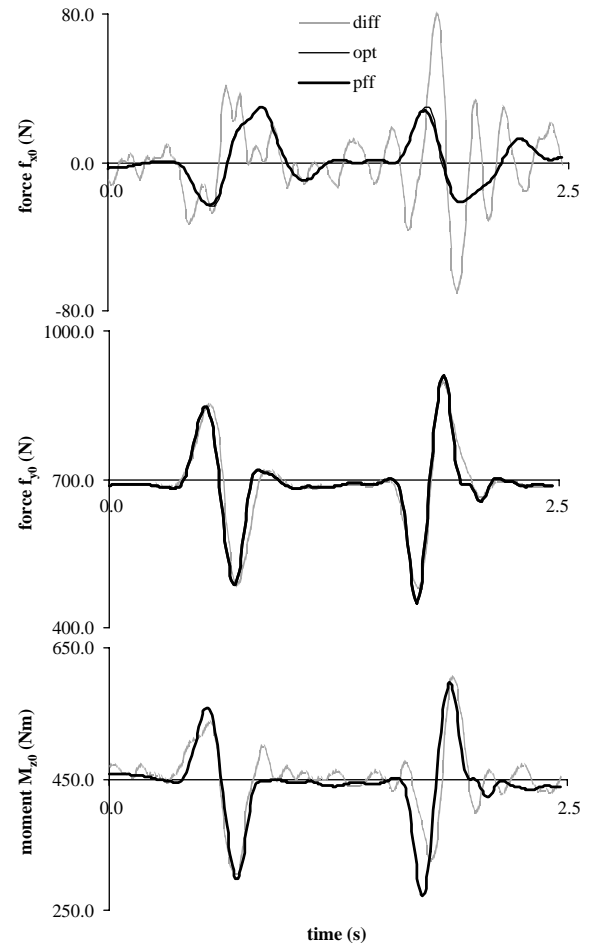


Fig. 3. Ground reactions. Horizontal and vertical forces (f_{x0} and f_{y0}) and moment (M_{z0}) estimated using double-differentiated position measurements (diff) or optimal accelerations (opt), along with force plate measurements (pff).

estimations of ground reaction components with a mean relative RMS of 0.5% compared to an average relative RMS deviation of 12% for the solutions obtained with numerically differentiated accelerations.

Optimal net joint moment estimations are obtained by solving the inverse dynamics problem using optimal accelerations. Large deviations can be observed between the joint moments calculated with the proposed method and those given by the 'PID' technique, with a mean absolute RMS of 22.6 Nm for all joints. These discrepancies are due to the great sensitivity of the 'PID' moment estimations to inaccuracies in numerically determined accelerations. Deviations between optimal joint moment solutions and 'bottom-up' calculations are smaller, with a mean absolute value of 5.6 Nm. They typically increase from the lower to the upper end. The optimal ankle moment is very close to the 'bottom-up' estimation (0.04 Nm) which is determined from force plate measurements regardless of accelerations (Eq. (1)). The absolute RMS error increases to 14 Nm at the top-most joint. The average

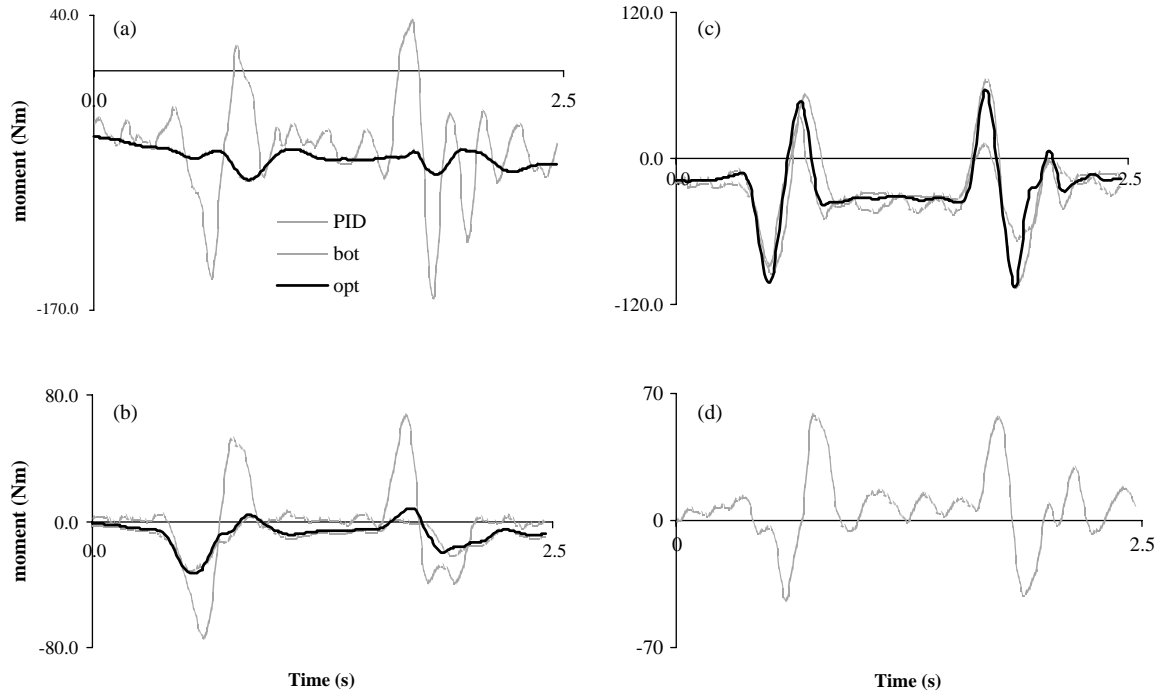


Fig. 4. Net joint moment calculations with classical methods using double-differentiated position measurements: pure inverse dynamics (PID) and bottom-up method (bot), and alternative method (opt) at each joints: ankle (a), hip (b) and shoulder (c). (The residual moment obtained with the bottom-up method at shoulder joint is represented in (d).)

residual moment induced by the ‘bottom-up’ approach reaches a maximum value of 58 N m (see Fig. 4d).

In conclusion, our method yields a set of optimal accelerations consistent with all available measurements. It accurately predicts ground reactions and produces no residual moment at the top-most segment. Optimal joint moment estimations can largely differ from classical calculations. Furthermore, the formulation is based on the over-determinacy of the system relating accelerations to measurements and performs even if some of the force measurements are missing. Finally, existing software packages based on the traditional inverse dynamics solution process can be readily improved by including the proposed least-squares optimisation as a separate subroutine.

Appendix A

For a four-body-segment model (Fig. 1), ankle joint reaction vector $\varphi_1 = \langle f_{x1}, f_{y1}, M_{z1} \rangle^T$ can be related to kinematic properties of upper segments ($i = 1-3$) (Eq. (2)). The elements of P , R and T are designated by lower case p , r and t , respectively, and require the preliminary definition of the following coefficients:

$$\begin{aligned} a_1 &= (m_1 r_1 + (m_2 + m_3) l_1), & b_1 &= (m_2 l_1 r_2 + m_3 l_1 l_2), \\ a_2 &= (m_2 r_2 + m_3 l_2), & \text{and } b_2 &= (m_3 l_1 r_3), \\ a_3 &= (m_3 r_3), & b_3 &= (m_3 l_2 r_3), \end{aligned}$$

$$\begin{aligned} p_{11} &= -(a_1 \cos \theta_1 + a_2 \cos (\theta_1 + \theta_2) + a_3 \cos (\theta_1 + \theta_2 + \theta_3)), \\ p_{12} &= -(a_2 \cos (\theta_1 + \theta_2) + a_3 \cos (\theta_1 + \theta_2 + \theta_3)), \\ p_{13} &= -a_3 \cos (\theta_1 + \theta_2 + \theta_3), \\ p_{21} &= -(a_1 \sin \theta_1 + a_2 \sin (\theta_1 + \theta_2) + a_3 \sin (\theta_1 + \theta_2 + \theta_3)), \\ p_{22} &= -(a_2 \sin (\theta_1 + \theta_2) + a_3 \sin (\theta_1 + \theta_2 + \theta_3)), \\ p_{23} &= -a_3 \sin (\theta_1 + \theta_2 + \theta_3), \\ p_{31} &= [(J_1 + r_1^2 m_1) + (J_2 + r_2^2 m_2) + (J_3 + r_3^2 m_3) \\ &\quad + (l_1^2 (m_2 + m_3) + l_2^2 m_3)], \\ &\quad + 2[b_1 \cos \theta_2 + b_2 \cos (\theta_2 + \theta_3) + b_3 \cos \theta_3], \\ p_{32} &= [(J_2 + r_2^2 m_2) + (J_3 + r_3^2 m_3) + (l_2^2 m_3)], \\ &\quad + [b_1 \cos \theta_2 + b_2 \cos (\theta_2 + \theta_3) + 2b \cos \theta_3], \\ p_{33} &= [(J_3 + r_3^2 m_3)] + [+b_2 \cos (\theta_2 + \theta_3) + b_3 \cos \theta_3], \end{aligned}$$

$$\begin{aligned} r_{11} &= -p_{21}, & t_{11} &= -2p_{22}, \\ r_{12} &= -p_{22}, & t_{12} &= -2p_{23}, \\ r_{13} &= -p_{23}, & t_{13} &= -2p_{23}, \\ r_{21} &= p_{11}, & t_{21} &= 2p_{12}, \\ r_{22} &= p_{12}, & \text{and } t_{22} &= 2p_{13}, \\ r_{23} &= p_{13}, & t_{23} &= 2p_{13}, \\ r_{31} &= 0, & t_{31} &= 2r_{32}, \\ r_{32} &= -[b_1 \sin \theta_2 + b_2 \sin (\theta_2 + \theta_3)], & t_{32} &= 2r_{33}, \\ r_{33} &= -[b_2 \sin (\theta_2 + \theta_3) + b_3 \sin \theta_3], & t_{33} &= 2r_{33}. \end{aligned}$$

Gravitational function f_g is expressed by

$$f_g(\theta) = -g[m_1(r_1 \sin \theta_1) + m_2(l_1 \sin \theta_1 + r_2 \sin (\theta_1 + \theta_2)) + m_3(l_1 \sin \theta_1 + l_2 \sin (\theta_1 + \theta_2) + r_3 \sin (\theta_1 + \theta_2 + \theta_3))]$$

Appendix B

According to the propagation law (Eq. (6)), variance components of s can be expressed as functions of standard measurement uncertainties $\Delta f_x, \Delta f_y, \Delta M_z$ and $\Delta \theta$

$$\Delta s_1^2 = \frac{\partial s_1}{\partial f_{x0}} \Delta f_x^2 + \sum_{i=1,n} \left(\frac{\partial s_1}{\partial \theta_i} + \frac{\partial s_1}{\partial \theta_{i-\Delta t}} + \frac{\partial s_1}{\partial \theta_{i+\Delta t}} \right) \Delta \theta^2,$$

$$\Delta s_2^2 = \frac{\partial s_2}{\partial f_{y0}} \Delta f_y^2 + \sum_{i=1,n} \left(\frac{\partial s_2}{\partial \theta_i} + \frac{\partial s_2}{\partial \theta_{i-\Delta t}} + \frac{\partial s_2}{\partial \theta_{i+\Delta t}} \right) \Delta \theta^2,$$

$$\Delta s_3^2 = \frac{\partial s_3}{\partial f_{x0}} \Delta f_x^2 + \frac{\partial s_3}{\partial f_{y0}} \Delta f_y^2 + \frac{\partial s_3}{\partial M_{z0}} \Delta M_z^2 + \sum_{i=1,n} \left(\frac{\partial s_3}{\partial \theta_i} + \frac{\partial s_3}{\partial \theta_{i-\Delta t}} + \frac{\partial s_3}{\partial \theta_{i+\Delta t}} \right) \Delta \theta^2,$$

$$\Delta s_k^2 = \sum_{i=1,n} \left(\frac{\partial s_k}{\partial \theta_i} + \frac{\partial s_k}{\partial \theta_{i-2\Delta t}} + \frac{\partial s_k}{\partial \theta_{i+2\Delta t}} \right) \Delta \theta^2.$$

For a four-body-segment model (Fig. 1), $\Delta s_{i=1,6}^2$ are defined, respectively, by

$$\Delta s_1^2 = \Delta f_x^2 + \left(\sum_{i=1,3} \alpha_{i1}^2 + 2\Delta f e^2 \sum_{i=1,3} \beta_{1i}^2 \right) \Delta \theta^2,$$

$$\Delta s_2^2 = \Delta f_y^2 + \left(\sum_{i=1,3} \alpha_{i2}^2 + 2\Delta f e^2 \sum_{i=1,3} \beta_{2i}^2 \right) \Delta \theta^2,$$

$$\Delta s_3^2 = l_0^2 \Delta f_x^2 + d_0^2 \Delta f_y^2 + \Delta M_z^2 + \left(\sum_{i=1,3} \left(\alpha_{i3} + \frac{\partial f_g}{\partial \theta_i} \right)^2 + 2\Delta f e^2 \sum_{i=1,3} \beta_{3i}^2 \right) \Delta \theta^2,$$

$$\Delta s_k^2 = \left(\frac{3\Delta f e^4}{8} \right) \Delta \theta^2,$$

where α_k and β_k are vectors given by

$$\alpha_k = \Delta R_k \dot{\theta}^2 + \Delta T_k \dot{\theta} \dot{\theta} \quad \text{and} \quad \beta_k = U_k \dot{\theta}$$

with

$$\Delta R_k = \begin{bmatrix} \partial r_{ij} \\ \partial \theta_k \end{bmatrix}, \quad \Delta T_k = \begin{bmatrix} \partial t_{ij} \\ \partial \theta_k \end{bmatrix}$$

and

$$U_k = \begin{bmatrix} r_{k1} & t_{k1}/2 & t_{k2}/2 \\ r_{k2} & t_{k1}/2 & t_{k3}/2 \\ r_{k3} & t_{k1}/2 & t_{k3}/2 \end{bmatrix},$$

where r_{ij} and t_{ij} are components of, respectively, centrifugal and Coriolis' matrices defined in Appendix A.

References

- Andrews, J.G., 1995. Euler's and Lagrange's equations for linked rigid-body models of three-dimensional human motion. In: Allard, P., Stokes, I., Bianchi, J.P. (Eds.), *Three-Dimensional Analysis of Human Movement*. Human Kinetics, Leeds, pp. 145–175.
- Cappozzo, A., Leo, T., Pedotti, A., 1975. A general computing method for the analysis of human locomotion. *Journal of Biomechanics* 8, 307–320.
- Challis, J.H., Kerwin, D.G., 1996. Quantification of the uncertainties in resultant joint moments computed in a dynamic activity. *Journal of Sports Sciences* 14, 219–231.
- Chao, E.Y., Rim, K., 1973. Application of optimisation principles in determining the applied moments in human leg joints during gait. *Journal of Biomechanics* 6, 497–510.
- Ciarlet, P.G., 1994. Généralités sur l'optimisation. In: *Introduction à l'analyse numérique matricielle et à l'optimisation*. Masson, Paris, pp. 167–206.
- Eng, J.J., Winter, D.A., MacKinnon, C.D., Patla, A.E., 1992. Interaction of the reactive moments and centre of mass displacement for postural control during voluntary arm movements. *Neuroscience Research Communications* 11, 73–80.
- Hatze, H., 2000. The inverse dynamics problem of neuromuscular control. *Biological Cybernetics* 82, 133–141.
- ISO Guide to the expression of uncertainty in measurement, 1993. Geneva.
- Kuo, A.D., 1998. A least-squares estimation approach to improving the precision of inverse dynamics computations. *Journal of Biomechanical Engineering-ASME* 120, 148–159.
- Kuo, A.D., Zajac, F.E., 1993. Human standing posture: multi-joint movement strategies based on biomechanical constraints. In: Allum, J.H., Allum-Mecklenburg, D.J., Harris, F.P., Probst, R. (Eds.), *Progress in Brain Research*, Vol. 97. Amsterdam, Elsevier, pp. 349–358.
- Späegele, T., Kistner, A., Gollhofer, A., 1999. Modelling, simulation and optimisation of a human vertical jump. *Journal of Biomechanics* 32, 521–530.
- Vaughan, C.L., Andrews, J.G., Hay, J.G., 1982. Selection of body segment parameters by optimisation methods. *Journal of Biomechanical Engineering-ASME* 104, 38–44.
- Winter, D.A., 1990. *Biomechanics and Motor Control of Human Movement*. Wiley-Interscience, New York.
- Woltring, H.J., 1990. Model and measurement error influences in data processing. In: Berme, N., Cappozzo, A. (Eds.), *Biomechanics of Human Movement*. Bertec Corporation, USA, pp. 203–237.
- Wood, G.A., 1982. Data smoothing and differentiation procedures in biomechanics. *Exercise and Sport Sciences Reviews* 10, 308–362.
- Zajac, F.E., 1993. Muscle coordination of movement: a perspective. *Journal of Biomechanics* 26, 109–124.
- Zajac, F.E., Gordon, M.E., 1989. Determining muscle's force and action in multi-articular movement. *Exercise and Sport Science Reviews* 17, 187–230.